Journal of Instrumentation

Radiation hardness and timing studies of a monolithic TowerJazz pixel design for the new ATLAS Inner Tracker

To cite this article: C. Riegel *et al* 2017 *JINST* **12** C01015

Published by IOP Publishing for Sissa Medialab

Received: *September 30, 2016*
Revised: *December 9, 2016*
Accepted: *December 13, 2016*
Published: *January 3, 2017*

18th International Workshop on Radiation Imaging Detectors
3–7 July 2016,
Barcelona, Spain

Radiation hardness and timing studies of a monolithic TowerJazz pixel design for the new ATLAS Inner Tracker

C. Riegel,[a,b,1] **M. Backhaus,**[a,2] **J.W. Van Hoorne,**[a] **T. Kugathasan,**[a] **L. Musa,**[a] **H. Pernegger,**[a] **P. Riedler,**[a] **D. Schaefer,**[a] **W. Snoeys**[a] **and W. Wagner**[b]

[a] *CERN,*
385, route de Meyrin, Meyrin, Switzerland
[b] *University of Wuppertal,*
Gaußstraße 20, Wuppertal, Germany

E-mail: Christian.Riegel@cern.ch

Abstract: A part of the upcoming HL-LHC upgrade of the ATLAS Detector is the construction of a new Inner Tracker. This upgrade opens new possibilities, but also presents challenges in terms of occupancy and radiation tolerance. For the pixel detector inside the inner tracker, hybrid modules containing passive silicon sensors and connected readout chips are presently used, but require expensive assembly techniques like fine-pitch bump bonding. Silicon devices fabricated in standard commercial CMOS technologies, which include part or all of the readout chain, are also investigated offering a reduced cost as they are cheaper per unit area than traditional silicon detectors. If they contain the full readout chain, as for a fully monolithic approach, there is no need for the expensive flip-chip assembly, resulting in a further cost reduction and material savings. In the outer pixel layers of the ATLAS Inner Tracker, the pixel sensors must withstand non-ionising energy losses of up to 10^{15} n/cm^2 and offer a timing resolution of 25 ns or less. This paper presents test results obtained on a monolithic test chip, the TowerJazz 180 nm Investigator, towards these specifications. The presented program of radiation hardness and timing studies has been launched to investigate this technology's potential for the new ATLAS Inner Tracker.

Keywords: Particle tracking detectors (Solid-state detectors); Radiation damage to detector materials (solid state); Radiation-hard detectors

[1]Corresponding author.
[2]Now ETH Zurich, Rämistrasse 101, Zurich, Switzerland.

doi:10.1088/1748-0221/12/01/C01015

2017 JINST 12 C01015

Contents

1 Introduction

The present ATLAS tracking system is performing an outstandingly good job in tracking, reconstructing and identifying of particles. Being the first detector system around the interaction point, the silicon pixel layers play a crucial part. Starting at around 2024 the High Luminosity LHC (HL-LHC) will deliver an additional 2500 fb^{-1} to the ATLAS detector at an instantaneous luminosity of $5{\times}10^{34}$ cm^{-2}s^{-1} [1]. The much higher radiation requirements and occupancy conditions of the HL-LHC demand a complete replacement of the current tracking system. The new ATLAS Inner Tracker (ITk) will consist of five layers of silicon pixel sensors and four double-layers of silicon strip sensors around the beam pipe.

In silicon detectors two quantities play an important role as far as radiation damage is concerned: the Total Ionising Dose (TID) and the 1 MeV neutron equivalent fluence (NIEL). The radiation requirements for the ITk Pixel sensors differ between sensors in the inner layers ($R < 6$ cm) and in the outer layers ($R < 26$ cm). The 1 MeV neutron-equivalent fluences are shown in figure 1, normalised to 3000 fb^{-1}. In the center of the innermost pixel layer, sensors need to tolerate $1.4{\times}10^{16}$ n/cm^2 and 7.7 MGy, in case of the outer pixel barrels, the maximum fluence and dose are $1.7{\times}10^{15}$ n/cm^2 and 0.9 MGy at the end of layer 3 [1].

2 Monolithic active pixel sensors (MAPS) — TowerJazz Investigator test chip

Sensors — pixels as well as strips — fabricated in commercial CMOS processes have been investigated to reduce cost when equipping several square meters in the new ITk. In case of monolithic active pixel sensors (MAPS) all functionality of the readout (sensor as well as front-end) would be embedded into one chip. This approach significantly simplifies the assembly [2]. In traditional MAPS, diffusion as opposed to drift is an important component of the collection of signal charge, and it is well known [7] that after significant non-ionising irradiation only drift is effective to collect the signal charge before it is captured by the radiation-induced traps. Charges deposited inside a depleted volume are collected by drift and generate fast signal responses needed to fulfil the

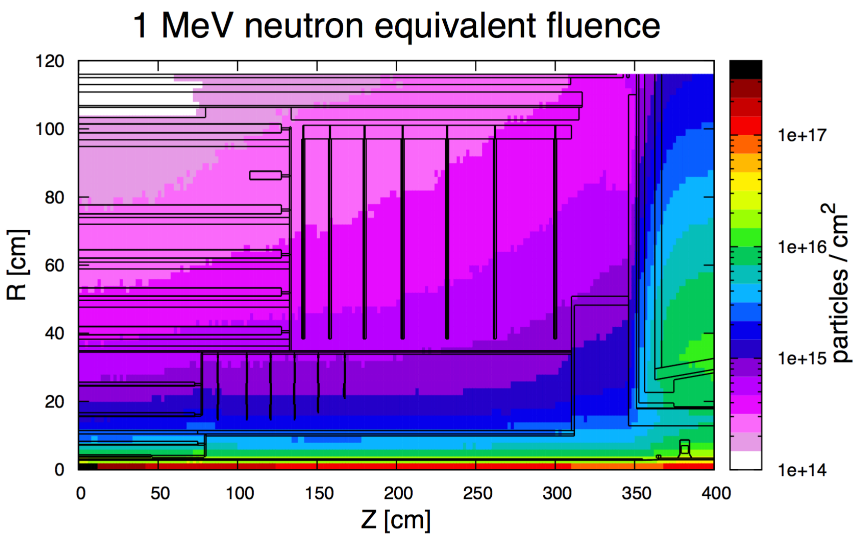

Figure 1. Expected 1 MeV neutron equivalent fluence in the ATLAS ITk normalised to 3000 fb^{-1} generated using PYTHIA8. For the outer pixel barrels, the maximum fluence is 1.7×10^{15} n/cm^2 [1].

required timing resolution of less than 25 ns. For high efficiency, the sensor therefore should reach complete lateral depletion in its high radiation environment. In the following results are presented for MAPS for which the process has been adapted. This new process modification aims to improve the depletion of the sensitive layer after irradiation. This way, signal charge collection by drift is enhanced to fulfil the timing requirements of the ATLAS ITk.

The TowerJazz Investigator is one chip out of a series of test chips designed for the upgrade of the ALICE Inner Tracking System (ITS) produced in the TowerJazz 180 nm technology [3, 4]. The chip allows the study of the signal shape (amplitude and analog timing) and charge sharing behavior. In total 134 different pixel matrices are available in the chip with pixel sizes from 20 μm to 50 μm. A cross section of the chip (standard process) is shown in figure 2a: using the deep Pwell as shield, CMOS circuits can be implemented in the pixel. By applying a negative HV to Deep Pwell and P-Substrate with respect to the collection electrode, a region in the epitaxial layer gets depleted as indicated in white [3]. The pixel matrices of the TowerJazz Investigator chip differ with respect to collection-diode geometries (combinations of different pixel sizes, electrode sizes and spacing) as well as different pixel reset mechanisms (active transistor reset or continuous diode reset). As shown in figure 2b, each of those matrices contains 8×8 active pixels surrounded by one line of inactive dummy pixels to separate different matrices against each other, reducing edge effects. Those pixels are biased in the same way but are not further connected. The results presented here had been obtained on chips with an epitaxial layer thickness of 25 μm. The measurements were done for a matrix with 50 μm pixel pitch, collection electrode of 3 μm size and a spacing of 20 μm. A matrix using an active transistor reset has been used to obtain fast signal responses.

The samples of the modified process used in the presented measurements had been irradiated in Ljubljana (TRIGA) with 1 MeV neutrons.[1] This radiation campaign included several irradiation steps (1.7×10^{13} n/cm^2, 4.0×10^{13} n/cm^2, 1.0×10^{14} n/cm^2, 2.0×10^{14} n/cm^2, $4.0. \times 10^{14}$ n/cm^2,

[1]Irradiation done with support of the AIDA2020 project.

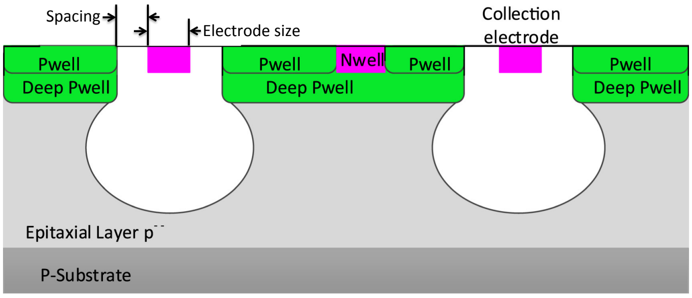

(a) Cross section of sensor technology (standard process, not to scale).

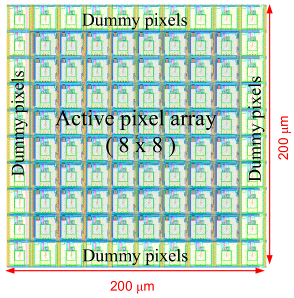

(b) Pixel matrix of 8×8 pixels surrounded by dummy pixels,

Figure 2. (a) Cross section of the monolithic active pixel sensor (standard process). The pixel geometries available in the Investigator chip differ in pixel size and also in electrode size and spacing. (b) Each selectable matrix contains 8×8 active pixels surrounded by a row of dummy pixels to reduce edge effects between matrices. The picture shows a matrix with pixels of 20 μm pixel pitch [3].

$1.0{\times}10^{15}$ n/cm^2). Measurements so far concentrated on the samples irradiated to the maximum fluence.

3 Setup and analysis

The Investigator is glued and wire-bonded to a carrier board which supplies all inputs and outputs via PCIe connector except for the HV used to deplete the pixel volume. This HV supply is applied using a separate LEMO connector in the range of 0 V to −6 V to avoid break-throughs in the pixel electronics. In addition to a supply voltage of 1.8 V other inputs have to be provided for the operation of the Investigator: since the matrix under investigation requires a periodic reset, logic has been implemented in an FPGA to veto triggering on the pixel response during a time window around the reset pulse. In the performed measurements a reset voltage of −1 V had been used. Furthermore, four constant currents are used for source followers in the analog pixel circuit. The matrix under test is selected using an address given by nine bits. The signals of all 64 pixels of the selected matrix are available via the PCIe connector. The readout in the pixels is realised by follower circuits [3].

Biases, supply voltages and control signals are provided through a Multi-IO (MIO) board and a General Purpose Analog Card (GPAC). A custom-made adapter board has been designed to connect the Investigator carrier board and the GPAC. The logical reset signal is generated in the FPGA of the MIO board and the HV supply reverse biasing the substrate has been applied using an external power supply.

The adapter board in its current version can be equipped with up to 25 LEMO connectors. Each connector can be used to access the analog signal given by one pixel in the selected matrix. The connectors form a 5×5 grid resembling the position of the pixels. This way, it is planned to also record signals of neighbouring pixels in order to investigate charge sharing and cluster sizes. Results presented here are obtained in single-pixel measurements.

A climate chamber at −30 °C is used to reduce the leakage current in irradiated sensors. This is a crucial point since the oscilloscope triggers on the signal itself. In addition, both measurement and storage of irradiated sensors is done at low temperature to prevent annealing.

The analog output signals of the pixels are connected to a DRS4 Evaluation Board. The DRS4 is a fast USB oscilloscope equipped with four channels and capable of sampling up to 5 GS/s [5]. One channel is used for the reset veto created by the FPGA on the MIO board in order to prevent triggering on the reset response itself as shown in figure 3a: here, the red curve is the waveform recorded by an oscilloscope. The reset veto in black indicates two time frames containing resets. The pixel responds with very deep spikes. Vetoing these intervals enables to trigger only on hits which appear as steps proportional to the collected charge as seen between the reset intervals. The remaining three channels can be used for signals. The signals are amplified using inverting CIVIDEC C1 broadband amplifiers [6]. By doing so, resolution and signal/noise separation could be improved.

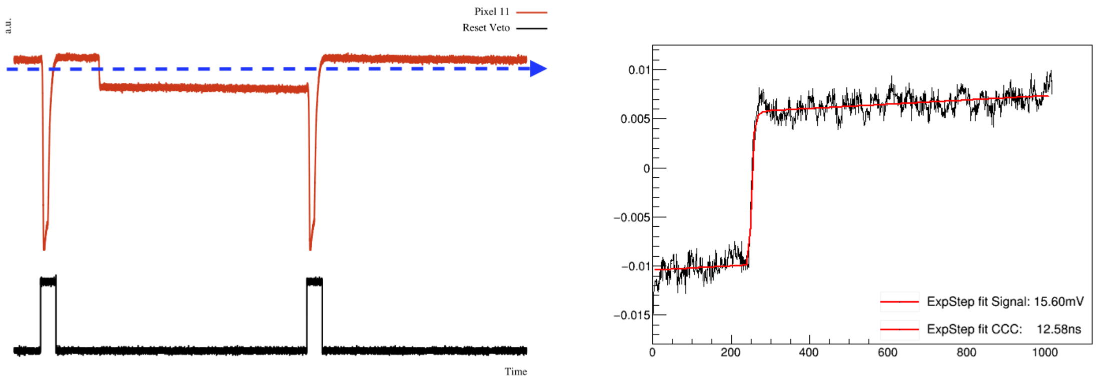

(a) Pixel response (uninverted, red) and reset veto (black),

(b) Waveform (inverted) with fit.

Figure 3. (a) Triggering is done directly on the pixel output (red) below the leakage level as indicated by the blue arrow. A reset veto (black) defines a time window around the reset to prevent triggering on the reset response. This data was recorded uninverted with a lab oscilloscope. (b) Once the waveform is recorded with the DRS4, an exponential fit is performed as described in the equations (3.1a) and (3.1b). This data was recorded in the setup using an inverting CIVIDEC amplifier and a DRS4.

The waveforms recorded by the DRS4 are analysed using the in-house software framework *tbConverter*. The procedure includes reading in the binary format of the DRS4 waveforms, applying first cuts to remove waveforms only containing noise and a fit to the remaining waveform. Procedure and fitting had already been performed successfully for the investigations of other technologies [7]. We adjusted the trigger in such a way that we record noise in addition to hits. An example waveform with applied fit is shown in picture 3b.

The fitted function is given in the equations (3.1a) and (3.1b) [7]. Before the time of the hit ($t \leq t_0$) a slope is used to fit the leakage current. The hit itself is described by adding an exponential function for $t > t_0$. We interpret the step parameter b as amplitude resulting in the deposited charges. We define the signal rise time as the time difference between 10 % and 90 % of the signal amplitude. Using the timing constant c of the exponential fit, this equals $(2.2 \cdot c)$.

$$t \leq t_0 \qquad f = a + m \cdot (t - t_0) \tag{3.1a}$$

$$t > t_0 \qquad f = a + m \cdot (t - t_0) - b \cdot \left(e^{-\frac{t-t_0}{c}} - 1\right). \tag{3.1b}$$

4 Source measurements with ^{55}Fe and ^{90}Sr

For the results presented here two different radioactive sources, ^{55}Fe emitting x-rays and ^{90}Sr emitting Minimum Ionising Particles (MIPs) have been used. Scans on unirradiated and irradiated devices have been carried out under the same conditions to allow comparison. Only the trigger threshold is individually adapted to the gain of the sample and the duration of the scans was not constant. This results in unequal numbers of recorded waveforms per scan.

A single-pixel ^{55}Fe spectrum obtained in a measurement for a pixel of 50 μm size with a collection electrode of 3 μm and an applied HV of −6 V is shown in figure 4a. The peak of ^{55}Fe is clearly visible as well as shared hits having a lower amplitude. The comparison between the spectrum of the unirradiated sample in black and the sample irradiated to 10^{15} n/cm^2 in red shows a gain reduction of almost 20 % after irradiation. Despite this reduction the spectrum contains a clearly distinct peak even after this level of radiation. In the ^{55}Fe spectrum the mean value of the Gaussian fit corresponds to 5.9 keV energy deposited in the pixel. Using the energy of 3.6 eV needed to create an electron-hole pair [8] in silicon spectra of MIPs are then converted into electrons. This procedure ensures that changes in gain due to irradiation as observed are taken into account.

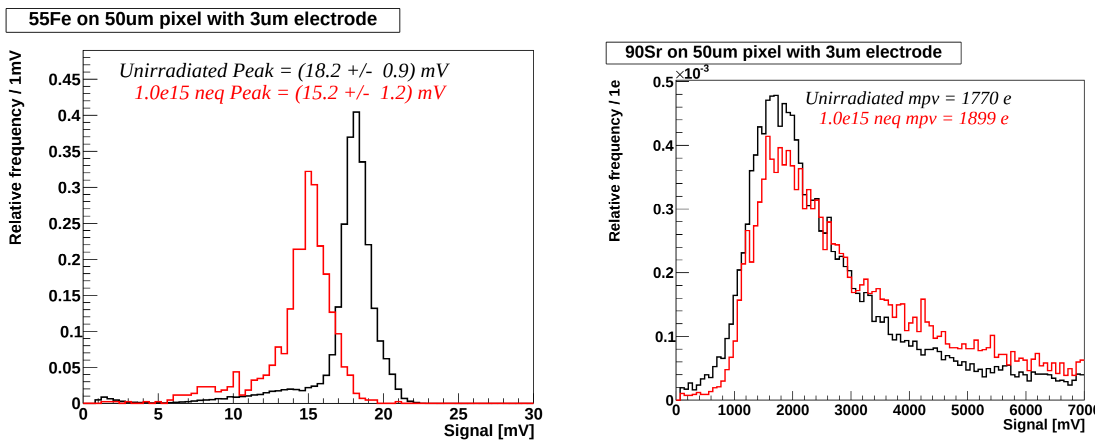

(a) Single-pixel ^{55}Fe spectrum.

(b) Single-pixel ^{90}Sr spectrum, calibrated.

Figure 4. (a) Single-pixel spectra obtained for the source measurements using (a) ^{55}Fe and (b) ^{90}Sr sources: for both the unirradiated sample (black) and the sample irradiated to 10^{15} n/cm^2 (red) a clear peak is visible with additional hits to lower signal sizes in the ^{55}Fe spectrum. The ^{90}Sr spectrum has been converted into electrons using the corresponding ^{55}Fe peak positions. For both the unirradiated sample (black) and the sample irradiated to 10^{15} n/cm^2 (red) the distributions follow a clear landau shape.

To obtain a MIP spectrum, the measurement is repeated with a ^{90}Sr source. The waveforms are recorded and analysed in the same way. The converted single-pixel spectrum of the ^{90}Sr tests is shown in figure 4b. Both spectra — again unirradiated in black an irradiated in red — show a landau distribution. After the applied gain calibration the MPVs obtained using a landau fit are 1777 e before and 1899 e after irradiation. Regarding the uncertainties given by the ^{55}Fe peak positions — 5 % before and 8 % after irradiation — and by the statistics of the measurements, the values agree with the expectation for an effective thickness of the depleted part of the epitaxial layer of somewhat less than 25 μm under the assumption of 80 $\frac{e}{\mu m}$ for the MPV: 80 $\frac{e}{\mu m} \cdot \sim$23 μm=1840 e.

2017 JINST 12 C01015

The second parameter in focus beside the radiation hardness is the timing of the signals. As described above, the timing information is obtained using the fit parameter of the exponential decay constant in equation (3.1b). Figure 5 shows a histogram of the calculated signal rise times for the waveforms corresponding to the ^{90}Sr spectra shown in figure 4b. Having again unirradiated in black and irradiated in red, the comparison of both histograms shows a slight increase in the signal rise time of around 15.5 % from (16.0 ± 3.2) ns to (18.5 ± 4.1) ns. Still, both signal rise times are lower than one bunch crossing time of 25 ns. Comparing the RMS of both timing distributions shows that also the spread of the signal rise time increases with radiation.

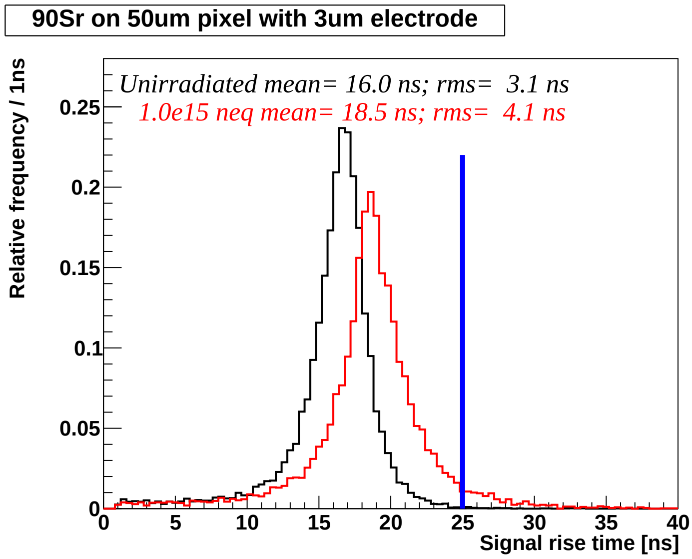

Figure 5. Signal rise time for the hits of the ^{90}Sr spectrum shown in 4b: compared to the unirradiated sample (black), the sample irradiated to 10^{15} n/cm^2 (red) has a slightly higher signal rise time and a wider distribution. Both means are below 25 ns as indicated by the blue line.

The timing distributions of figure 5 plotted against the ^{90}Sr amplitude spectra of figure 4b are shown before irradiation in figure 6a and after irradiation in figure 6b. After irradiation, the general shape of the distribution stays the same but as already observed before, the distribution slightly widens in time. It seems to effect hits of all amplitudes and not only a specific amplitude range.

In previous measurements of silicon sensors after irradiation, diffusion contributions are present before irradiation and vanish after irradiation due to charge trapping [7]. None of the distributions show a large tail indicating only a small contribution of diffusion to the charge collection.

The degradation after irradiation is not very significant either. All this provides a strong hint that a significant fraction of the sensitive volume is depleted with the 6 V applied, yielding the collection of a very significant fraction of the signal charge in a short time resulting in small signal rise times.

5 Summary and outlook

The results presented here analyse the radiation hardness of a monolithic CMOS pixel sensor produced in the TowerJazz 180 nm technology for the future ATLAS Inner Tracker. The single-pixel measurements of samples of the modified process for enhanced depletion show that the spectra

2017 JINST 12 C01015

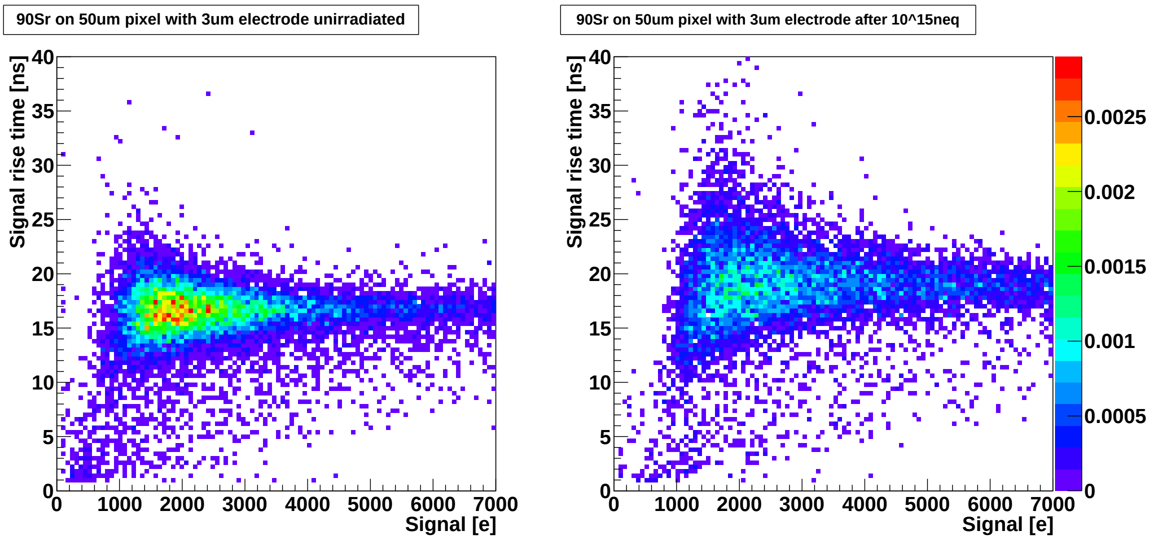

(a) Unirradiated sample. **(b)** Sample after irradiation.

Figure 6. Signal rise time plotted against the signal size of the ^{90}Sr spectra for (a) the unirradiated sample and (b) the sample after 10^{15} n/cm^2: as seen in the single distributions, the shape stays the same but a further spread in the signal rise time is visible.

of both x-rays and MIPs can be recorded and observed even after irradiation to 1.0×10^{15} n/cm^2 . Effects of the irradiation can be seen in a reduction of gain of almost 20 % and an increase in the signal rise time of around 15.5 %. Plotting the distributions of signal rise time and amplitude versus each other shows that the increase of the signal rise time is not an effect limited only to certain amplitude ranges but can be observed over the entire amplitude spectrum.

Even before radiation, no diffusion component of high timing values is visible. This is a strong indication that the epitaxial layer is highly depleted for the applied HV of −6 V.

A new radiation campaign is ongoing in order to further investigate the limits of the technology in terms of radiation damage. Samples of the TowerJazz Investigator will be irradiated up to 1.0×10^{16} n/cm^2 including intermediate values. The newly irradiated samples will be treated and tested under the same conditions using again both ^{55}Fe and ^{90}Sr sources. The data obtained by those measurements will give further inside on the impact of radiation damage in the epitaxial volume on amplitude and timing.

In addition an ongoing test beam at the CERN SPS using pions will provide information concerning the efficiency before and after radiation also in dependence of applied bias voltage. The setup had been adapted to read out up to 11 pixels simultaneously. This development increases the obtained data rate and also provides additional information beyond the presented single-pixel spectra.

Acknowledgments

The authors want to thank the CERN EP-EPS design team for providing detailed information whenever it was needed as well as I. Mandic and his team from Ljubljana for the support of irradiated samples.

2017 JINST 12 C01015

The work is sponsored by the Wolfgang Gentner Programme of the Federal Ministry of Education and Research (Germany) and supported by the H2020 project AIDA-2020, GA no. 654168.

References

[1] ATLAS collaboration, *Letter of Intent for the Phase-II Upgrade of the ATLAS Experiment*, CERN-LHCC-2012-022 (2012).

[2] G. Aglieri et al., *Monolithic active pixel sensor development for the upgrade of the ALICE inner tracking system*, 2013 *JINST* **8** C12041.

[3] C. Gao et al., *A Novel Source-Drain Follower for Monolithic Active Pixel Sensors*, proceedings of the *10th International 'Hiroshima' Symposium on the Development and Application of Semiconductor Tracking Detectors (HSTD-10)*, Xian, China, 25–29 September 2015 [*Nucl. Instrum. Meth.* **A 831** (2016) 147].

[4] J.W. van Hoorne, M. Krammer amd P. Riedler, *Study and Development of a novel Silicon Pixel Detector for the Upgrade of the ALICE Inner Tracking System*, Ph.D. Thesis, Technische Universität Wien, Wien Austria (2015) [CERN-THESIS-2015-255].

[5] S. Ritt, *Development of high speed waveform sampling ASICs*, proceedings of the *DAE-BRNS national symposium on nuclear instrumentation*, Mumbai, India, 24–26 February 2010 https://www.psi.ch/drs/evaluation-board.

[6] CIVIDEC Instrumentation GmbH, www.cividec.at.

[7] S. Fernandez-Perez et al., *Charge collection properties of a depleted monolithic active pixel sensor using a HV-SOI process*, 2016 *JINST* **11** C01063.

[8] K.G. McKay and K.B. McAfee, *Electron Multiplication in Silicon and Germanium*, *Phys. Rev.* **91** (1953) 1079.

2017 JINST 12 C01015